Title

A new family of quadrilateral thick plate finite elements based on linked interpolation

Authors

Auricchio, Ferdinando
Taylor, Robert

Publication Date

1993-10-01

REPORT NO.
UCB/SEMM-93/10

STRUCTURAL ENGINEERING,
MECHANICS AND MATERIALS

A NEW FAMILY OF QUADRILATERAL THICK PLATE FINITE ELEMENTS BASED ON LINKED INTERPOLATION

by

FERDINANDO AURICCHIO

ROBERT L. TAYLOR

October 1993

DEPARTMENT OF CIVIL ENGINEERING
UNIVERSITY OF CALIFORNIA
BERKELEY, CALIFORNIA

A NEW FAMILY OF QUADRILATERAL THICK PLATE FINITE ELEMENTS BASED ON LINKED INTERPOLATION

F.Auricchio R.L.Taylor
Department of Civil Engineering
University of California at Berkeley, Berkeley, CA 94720 USA

Abstract

We present a new family of quadrilateral finite elements developed within the framework of a shear deformable plate theory. All the elements take advantages of the so-called *linked* interpolation, i.e. an higher order interpolation for the transverse displacement is obtained using the discrete parameters of the rotational field. Based on an extensive set of mixed patch tests, a careful study of the element behaviors is performed. Moreover, the results for a large group of standard numerical examples are presented, together with the results from three other elements available in the literature. All the elements show proper rank, good interpolating capacity and no locking effects in the limiting case of thin plate.

1 INTRODUCTION

In the development of a planar beam element within the context of Euler-Bernoulli theory, it has always been considered natural to introduce three degrees of freedom at each node (the two in-plane displacements and one rotation) and include a contribution of the nodal rotations to the transverse displacement, i.e. to *link* the transverse displacement field to the discrete nodal rotations. This is usually done to guarantee an higher order polynomial in the transverse displacement than in the rotations, as required since the latter are just the derivative of the former. However the use of linked interpolation leads to even more important properties in the case of shear deformable beams, as presented in References [25, 26] and discussed in Section 4 of this work: it in fact allows for constant shear strain, hence avoiding locking effects in the limiting thin case.

Despite such interesting conclusion derived within a one-dimensional beam theory, the corresponding two-dimensional analogue has never been explored too deeply. Examples of two dimensional theories in which the displacement field is linked to the nodal rotational parameters can be found in literature for the case of plane elasticity analysis [1], while examples for bending problems can be found in the work of Auricchio and Taylor [2], Taylor and Auricchio [27], Zienkiewicz et al. [36], Xu [31, 32], Xu et al. [33].

The paper is organized as follow. We start with a brief overview of the linear elastic shear deformable plate theory adopted, with an appropriate variational framework. After that, we introduce a mixed finite element approximation together with the requirements for the convergence of the formulation; we also discuss a complete series of mixed patch tests which allow to assess the quality of the interpolation scheme. We then describe a new family of finite elements developed within the plate theory previously addressed and present the results both for the patch tests and a large set of standard numerical tests. In order to make appropriate evaluation of the performance of the elements proposed, we also report the results for other three finite elements available in literature.

2 A linear thick plate theory

Early developments of a thick plate theory, which include both bending deformation and the primary effects of transverse shear deformation, are commonly attributed to Mindlin [14] and Reissner [20]. The theory presented here is a simplification of those originally proposed and due to its simplicity it can be thought either as a degeneration from the three-dimensional elasticity theory or as an example of the the so-called *direct approach* [8, 15, 21, 22].

Geometry and load

With the term *plate* we refer to a flat thin body, occupying the domain:

$$\Omega = \left\{ (x,y,z) \in \mathcal{R}^3 \mid z \in \left[-\frac{h}{2}, +\frac{h}{2} \right], (x,y) \in \mathcal{A} \subset \mathcal{R}^2 \right\}$$

where the plane $z = 0$ coincides with the mid-surface of the undeformed plate and the transverse dimension, or *thickness* h, is small compared to the other two dimensions. Furthermore, the loading is restricted to be applied only in the direction normal to the mid-surface.

Kinematics

Limiting the discussion to the realm of infinitesimal kinematics, we assume that:

$$\begin{aligned} u(x,y,z) &= z\theta_y(x,y) \\ v(x,y,z) &= -z\theta_x(x,y) \\ w(x,y,z) &= w(x,y) \end{aligned} \tag{2.1}$$

where u, v and w are the displacements along the x, y and z axes, respectively, and θ_x and θ_y are the rotations of the transverse line elements about the x and y axes. Accordingly, a straight line element, normal to the plate mid-surface in the undeformed configuration, remains straight, but not necessarily normal to the deformed mid-surface, allowing for transverse shear deformations. As a direct consequence of equation 2.1, we may introduce a (generalized) *displacement* vector $\mathbf{u}$ with components:

$$\mathbf{u} = \left\{ \begin{array}{c} w \\ \theta_x \\ \theta_y \end{array} \right\} = \left\{ \begin{array}{c} w \\ \boldsymbol{\theta} \end{array} \right\}$$

The basic kinematic ingredients are the curvature, $\mathbf{K}$, and the shear strain, $\mathbf{\Gamma}$, defined as:

$$\begin{aligned} \mathbf{K} &= \left\{ \begin{array}{c} \kappa_{xx} \\ \kappa_{yy} \\ \kappa_{xy} \end{array} \right\} = \left\{ \begin{array}{c} \theta_{y,x} \\ -\theta_{x,y} \\ \theta_{y,y} - \theta_{x,x} \end{array} \right\} \\ \mathbf{\Gamma} &= \left\{ \begin{array}{c} \gamma_{xz} \\ \gamma_{yz} \end{array} \right\} = \left\{ \begin{array}{c} \theta_y + w_{,x} \\ -\theta_x + w_{,y} \end{array} \right\} \end{aligned}$$

which can be collected in a (generalized) *strain* $\mathbf{E}$:

$$\mathbf{E} = \left\{ \begin{array}{c} \mathbf{K} \\ \mathbf{\Gamma} \end{array} \right\}$$

Both the curvature and the shear strain can be expressed in terms of w and $\boldsymbol{\theta}$ as follow:

$$\mathbf{K} = \mathbf{L}\boldsymbol{\theta} \quad , \quad \mathbf{\Gamma} = [\mathbf{e}\boldsymbol{\theta} + \nabla w]$$

where:

$$\mathbf{L} = \begin{bmatrix} 0 & \dfrac{\partial}{\partial x} \\ -\dfrac{\partial}{\partial y} & 0 \\ -\dfrac{\partial}{\partial x} & \dfrac{\partial}{\partial y} \end{bmatrix} \quad , \quad \mathbf{e} = \begin{bmatrix} 0 & 1 \\ -1 & 0 \end{bmatrix} \quad , \quad \nabla = \left\{ \begin{array}{c} \dfrac{\partial}{\partial x} \\ \dfrac{\partial}{\partial y} \end{array} \right\}$$

with $\mathbf{L}$ and ∇ differential operators and $\mathbf{e}$ the so-called alternating matrix. As a consequence of the kinematic assumptions, we may distinguish between in-plane bending strains (ϵ_x, ϵ_y, γ_{xy}) and transverse shear strains (γ_{xz}, γ_{yz}). In the thin plate theory the transverse shear strains are assumed to be zero, thus providing constraint equations which allow to express θ_x and θ_y as derivatives of the transverse displacement w. Conversely, in the thick plate theory we allow for non-zero shear deformations.

Stresses and stress resultants

Due to the predominant behavior associated with the two in-plane dimensions, the normal stress in the z direction is negligible compared to the other stresses; hence, we may assume:

$$\sigma_z = 0$$

Although this position is inconsistent with a general three-dimensional theory and is not present in the work by Reissner (where σ_z varies through the thickness), we may also adopt it since it does not influence the development of a viable finite element formulation.

Consistent with the strain behavior, we may distinguish between in-plane stresses $(\sigma_x, \sigma_y, \tau_{xy})$ and transverse shears (τ_{xz}, τ_{yz}). Their integration through the thickness defines the stress resultants per unit length:

$$M_x = \int_{-\frac{h}{2}}^{\frac{h}{2}} \sigma_x z dz \quad , \quad M_y = \int_{-\frac{h}{2}}^{\frac{h}{2}} \sigma_y z dz \quad , \quad M_{xy} = \int_{-\frac{h}{2}}^{\frac{h}{2}} \tau_{xy} z dz$$

$$S_x = \int_{-\frac{h}{2}}^{\frac{h}{2}} \tau_{xz} dz \quad , \quad S_y = \int_{-\frac{h}{2}}^{\frac{h}{2}} \tau_{yz} dz$$

For notational convenience, we collect the resultants in a (generalized) *stress* $\mathbf{\Sigma}$:

$$\mathbf{\Sigma} = \left\{ \begin{array}{c} \mathbf{M} \\ \mathbf{S} \end{array} \right\}$$

where:

$$\mathbf{M} = \left\{ \begin{array}{c} M_x \\ M_y \\ M_{xy} \end{array} \right\} \quad , \quad \mathbf{S} = \left\{ \begin{array}{c} S_x \\ S_y \end{array} \right\}$$

Constitutive relation

Assuming the material to be elastic, it is possible to derive a corresponding elastic stress-strain constitutive relation for the plate, in the form:

$$\mathbf{\Sigma} = \mathbf{D}\mathbf{E}$$

In particular, for the case of isotropic homogeneous plate, the previous relation can be specialized as:

$$\left\{ \begin{array}{c} \mathbf{M} \\ \mathbf{S} \end{array} \right\} = \left[\begin{array}{cc} \mathbf{D}_b & \mathbf{0} \\ \mathbf{0} & \mathbf{D}_s \end{array} \right] \left\{ \begin{array}{c} \mathbf{K} \\ \mathbf{\Gamma} \end{array} \right\}$$

where:

$$\begin{aligned} \mathbf{D}_b &= \frac{Eh^3}{12(1-\nu^2)} \left[\begin{array}{ccc} 1 & \nu & 0 \\ \nu & 1 & 0 \\ 0 & 0 & \frac{1}{2}(1-\nu) \end{array} \right] \\ \mathbf{D}_s &= kGh \left[\begin{array}{cc} 1 & 0 \\ 0 & 1 \end{array} \right] \end{aligned}$$

with E being the Young 's modulus, ν the Poisson ratio, G the shear modulus. Finally, k is a factor, introduced to correct the inconsistency between the transverse shear strain, which is constant throughout the thickness, and the shear stress, which is not constant; k depends on the plate properties and is often set equal to 5/6 for isotropic homogeneous plates.

3 VARIATIONAL STRUCTURE

As discussed in Reference [2], the elastic plate field equations can be derived from a functional Π, based on the potential energy principle for the bending and on the Hu-Washizu principle for the transverse shear energy:

$$\begin{aligned}\Pi(w,\boldsymbol{\theta},\boldsymbol{\Gamma},\mathbf{S}) = &\frac{1}{2}\int_A \left[\mathbf{K}^T(\boldsymbol{\theta})\,\mathbf{D}_b\mathbf{K}(\boldsymbol{\theta})\right] dA + \frac{1}{2}\int_A \left[\boldsymbol{\Gamma}^T\mathbf{D}_s\boldsymbol{\Gamma}\right] dA \\ &- \int_A \left[\mathbf{S}^T(\boldsymbol{\Gamma} - \nabla w - \mathbf{e}\boldsymbol{\theta})\right] dA + \Pi_{ext}\end{aligned}$$

where Π_{ext} describes the loads and the boundary effects. Taking the variation of Π with respect to $\boldsymbol{\Gamma}$, we get:

$$\int_A \delta\boldsymbol{\Gamma}^T(\mathbf{S} - \mathbf{D}_s\boldsymbol{\Gamma})\, dA = 0 \tag{3.1}$$

Depending on the desired approach to the problem, this equation can be satisfied in a strong or in a weak sense. Since we limit our discussion only to the case of linear elastic plate, we may choose to satisfy equation 3.1 in a strong (pointwise) sense; accordingly, we get:

$$\mathbf{S} = \mathbf{D}_s\boldsymbol{\Gamma} \quad \text{or} \quad \boldsymbol{\Gamma} = \mathbf{D}_s^{-1}\mathbf{S}$$

Substitution of this relation into Π returns a new functional:

$$\begin{aligned}\Pi_1(w,\boldsymbol{\theta},\mathbf{S}) = &\frac{1}{2}\int_A \left[\mathbf{K}^T(\boldsymbol{\theta})\,\mathbf{D}_b\mathbf{K}(\boldsymbol{\theta})\right] dA \\ &- \frac{1}{2}\int_A \left[\mathbf{S}^T\mathbf{D}_s^{-1}\mathbf{S}\right] dA + \int_A \left[\mathbf{S}^T(\nabla w + \mathbf{e}\boldsymbol{\theta})\right] dA + \Pi_{ext}\end{aligned}$$

where we use the fact that $\mathbf{D}_s^{-T} = \mathbf{D}_s^{-1}$. If we now take the variation with respect to $\mathbf{S}$, we get:

$$-\int_A \left[\delta\mathbf{S}^T\mathbf{D}_s^{-1}\mathbf{S}\right] dA + \int_A \left[\delta\mathbf{S}^T(\nabla w + \mathbf{e}\boldsymbol{\theta})\right] dA = 0$$

and a strong satisfaction of this equation returns the potential energy functional, leading to a classical displacement formulation. Since it is well from the literature that a displacement formulation is ill-conditioned in the limiting case of thin plate (generating the so called *locking*), we turn to a weak satisfaction of the functional Π_1.

4 A BEAM ELEMENT WITH TRANSVERSE SHEAR STRAINS

In the present section, following References [25, 26], we illustrate some of the interesting properties, that can be obtained through the use of linked interpolation. To make our point, we consider the simple case of a shear deformable beam. A displacement field for bending may be defined as:

$$u = z\theta(x) \quad , \quad w = w(x)$$

where x defines the axis of the beam, z is the coordinate in the transverse direction, u is the displacement in the x direction, θ is a rotation about the y axis, and w is the transverse displacement. The curvature and the transverse shear strain are given by:

$$\begin{aligned} \kappa &= \theta_{,x} \\ \gamma &= \theta + w_{,x} \end{aligned}$$

Linear isoparametric interpolation may be used for describing the element geometry:

$$\mathbf{x} = N^1(\xi)\hat{\mathbf{x}}^1 + N^2(\xi)\hat{\mathbf{x}}^2$$

where $\mathbf{x} = \{x, y\}$ and $\mathbf{x}^i = \{x^i, y^i\}^T$ are the nodal coordinates and the shape functions are defined as:

$$N^1(\xi) = \frac{1}{2}(1-\xi) \quad , \quad N^2(\xi) = \frac{1}{2}(1+\xi)$$

We can do a similar choice for the rotation field:

$$\theta = N^1(\xi)\hat{\theta}^1 + N^2(\xi)\hat{\theta}^2$$

where $\hat{\theta}^1$ and $\hat{\theta}^2$ indicates the nodal rotations. For the transverse displacement we want an higher order expression such to guarantee consistency between the transverse displacement and the rotations in the limiting case of thin beam, when the latter are just the derivative of the former; so we may add a hierarchical quadratic term to the linear field:

$$w = N^1(\xi)\hat{w}^1 + N^2(\xi)\hat{w}^2 + N^3(\xi)\Delta\hat{w}^3$$

where the $\hat{w}^i$ are the nodal transverse displacements. The shape function associated with the hierarchical degree of freedom is given by:

$$N^3(\xi) = (1 - \xi^2)$$

Accordingly, the curvature and the shear strain are:

$$\kappa = \frac{1}{L}(\hat{\theta}^2 - \hat{\theta}^1) \tag{4.1}$$

$$\gamma = \frac{1}{L}(\hat{w}^2 - \hat{w}^1) + \frac{1}{2}(\hat{\theta}^1 + \hat{\theta}^2) + \xi\left[\frac{1}{2}(\hat{\theta}^2 - \hat{\theta}^1) - \frac{4}{L}\Delta\hat{w}\right] \tag{4.2}$$

where L indicates the length of the bar. Note that the curvature is constant, whereas the shear strain is linear in ξ.

The equilibrium of the beam requires:

$$\begin{aligned} \frac{dS}{dx} + q &= 0 \\ \frac{dM}{dx} - S &= 0 \end{aligned}$$

where S is the transverse shear force resultant, M is the bending moment, and q is the transverse loading intensity per unit length. Thus, static equilibrium of a beam requires the shear to be related to the derivative of the moment. This is for example the case of a cantilever beam loaded by a concentrated end force, for which the shear is constant, whereas the bending moment varies linearly with length. Accordingly, for constant cross-section, the strains given by 4.1 and 4.2 lead to an inconsistency with the requirements of static equilibrium and using the above interpolation fields the solution will always be approximate, i.e. the presented formulation does not allow for constant shear strain in the presence of bending behavior. This phenomenon is reflected in a finite element analysis by locking of the element in the case of thin beams.

However, it is interesting to notice that the problem so far described can be by-passed with an appropriate choice of the hierarchical parameter $\Delta\hat{w}$. Requiring the vanishing of the term in brackets in equation 4.2 yields a *linked* interpolation for the transverse displacement:

$$\hat{w} = N^1(\xi)\hat{w}^1 + N^2(\xi)\hat{w}^2 + \frac{L}{8}N^3(\xi)(\hat{\theta}^2 - \hat{\theta}^1) \tag{4.3}$$

Using this new discrete field, the shear strain is now constant:

$$\gamma = \frac{1}{L}(\hat{w}^2 - \hat{w}^1) + \frac{1}{2}(\hat{\theta}^1 + \hat{\theta}^2)$$

and it can be shown that the corresponding stiffness matrix is identical to the one obtainable using a linear transverse displacement and a reduced 1-point integration.

The results given above are useful in constructing the displacement field interpolations for bending of plates in which shear strains are to be retained (e.g., see [28]). It is also very interesting to note that the use of a linked interpolation helps in terms of satisfaction of the mixed patch test (discussed in Section 6), which requires to have as few parameter as possible in the transverse displacement interpolation. This may be achieved either by using an inconsistent interpolation (e.g., the Heterosis element of Hughes and Cohen [10]) or by interpolations which use parameters of the other fields as enumerated above.

5 Mixed finite element solution

In the previous sections the equations governing a simple thick plate theory together with a variational formulation have been presented. We now discuss a solution strategy within the class of mixed finite elements.

Following a *mixed* approach, we approximate the fields w, $\boldsymbol{\theta}$ and $\mathbf{S}$ with independent interpolation schemes, in the following form:

$$\begin{aligned} w &= \mathbf{N}_w\hat{\mathbf{w}} + \mathbf{N}_{w\theta}\hat{\boldsymbol{\theta}} \\ \boldsymbol{\theta} &= \mathbf{N}_\theta\hat{\boldsymbol{\theta}} \\ \mathbf{S} &= \mathbf{N}_s\hat{\mathbf{S}} \end{aligned} \tag{5.1}$$

where:

$$\hat{\mathbf{w}} \ , \ \hat{\boldsymbol{\theta}} \ , \ \hat{\mathbf{S}}$$

are the degrees of freedom of the discretized system and:

$$\mathbf{N}_w \ , \ \mathbf{N}_{w\theta} \ , \ \mathbf{N}_\theta \ , \ \mathbf{N}_s$$

are sets of shape functions. Again note that the rotational field is used to increase the polynomial order of the displacement field and this is explicitly stated by the $\mathbf{N}_{w\theta}$ shape functions. As discussed in the introduction and explained in details for the simpler case of the beam in the previous section, we have basically three reasons for using linked interpolation:

- with an appropriate choice of the $\mathbf{N}_{w\theta}$ shape functions we are able to obtain a constant shear strain along each side of the finite element,
- we guarantee a higher order interpolation for the transverse displacement than for the rotational field, as is required for the thin plate situation, when the latter are simply the derivative of the former,
- we have a transverse displacement interpolation with as few nodal parameter as possible, which is required for a satisfaction of the mixed patch test, as discussed in the next section.

Within the framework of a thick plate theory, the same technique has been already used by the authors in References [2, 27], by Zienkiewicz et al. in Reference [36], by Xu in References [31, 32] and by Xu et al. in Reference [33].

After we introduce the interpolation schemes into Π_1, the minimization of the functional leads to the usual algebraic system:

$$\begin{bmatrix} \mathbf{0} & \mathbf{0} & \mathbf{A} \\ \mathbf{0} & \mathbf{K}_b & \mathbf{B} \\ \mathbf{A}^T & \mathbf{B}^T & -\mathbf{H} \end{bmatrix} \begin{Bmatrix} \hat{\mathbf{w}} \\ \hat{\boldsymbol{\theta}} \\ \hat{\mathbf{S}} \end{Bmatrix} = \begin{Bmatrix} \mathbf{f}_w \\ \mathbf{f}_\theta \\ \mathbf{0} \end{Bmatrix} \tag{5.2}$$

where:

$$\begin{aligned}
\mathbf{A} &= \int_A (\nabla \mathbf{N}_w)^T \mathbf{N}_s dA \\
\mathbf{B} &= \int_A (\nabla \mathbf{N}_{w\theta})^T \mathbf{N}_s dA + \int_A (\mathbf{e}\mathbf{N}_\theta)^T \mathbf{N}_s dA \\
\mathbf{K}_b &= \int_A (\mathbf{L}\mathbf{N}_\theta)^T \mathbf{D}_b (\mathbf{L}\mathbf{N}_\theta)\, dA \\
\mathbf{H} &= \int_A \mathbf{N}_s^T \mathbf{D}_s^{-1} \mathbf{N}_s dA
\end{aligned}$$

and $\mathbf{f}_w$ and $\mathbf{f}_\theta$ are the load and the boundary terms.

Choosing the interpolating function for the shear $\mathbf{S}$ to be linearly independent within each element, the shear parameters $\hat{\mathbf{S}}$ may be statically condense at the element level, resulting in a displacement-like formulation only in the $\hat{\mathbf{w}}$ and $\hat{\boldsymbol{\theta}}$ unknowns. Accordingly, the last row of the previous system of linear algebraic equations can be solved in terms of $\hat{\mathbf{S}}$:

$$\hat{\mathbf{S}} = \mathbf{H}^{-1}\mathbf{A}^T\hat{\mathbf{w}} + \mathbf{H}^{-1}\mathbf{B}^T\hat{\boldsymbol{\theta}}$$

and substitute back in the other two rows of the system, giving:

$$\begin{bmatrix} \mathbf{A}\mathbf{H}^{-1}\mathbf{A}^T & \mathbf{A}\mathbf{H}^{-1}\mathbf{B}^T \\ \mathbf{B}\mathbf{H}^{-1}\mathbf{A}^T & \mathbf{K}_b + \mathbf{B}\mathbf{H}^{-1}\mathbf{B}^T \end{bmatrix} \left\{ \begin{array}{c} \hat{\mathbf{w}} \\ \hat{\boldsymbol{\theta}} \end{array} \right\} = \left\{ \begin{array}{c} \mathbf{f}_w \\ \mathbf{f}_\theta \end{array} \right\}$$

6 Requirements for convergence of a mixed formulation

Convergence is the property by which the approximate solution obtained from a discrete scheme such as a finite element model converges to the exact solution for successive mesh refinements. *Consistency* and *stability* are sufficient requirements to imply convergence: consistency ensures that the discrete model reproduces the exact continuum model for the limiting case of infinite number of degrees of freedom, while stability ensures that the solution of the discrete system is unique and not ill-conditioned.

Within a standard displacement finite element approach, the stability can be tested by checking that the stiffness matrix has the appropriate rank, while consistency is verified by the patch test. The original patch test was introduced by Irons [6, 12] based on a physical reasoning and establish the capacity of the discrete model to exactly reproduce constant strain states for simple patches of elements. Thereafter, other works have elaborated on the meaning and the importance of the test [13, 19, 24, 29, 30].

The convergence of a mixed finite element scheme is however more complex to verify and the mathematical conditions to be satisfied is embedded in the work of Babuska [3, 4] and Brezzi [7], which are based on quite involving mathematical arguments. Willing to remain in a more physical framework, an extended version of the patch test viable for mixed formulations has been presented and discussed in literature [16, 17, 18]. Clearly, the results obtainable from this type of analysis are not comparable in term of completeness and robustness with a rigorous convergence analysis, but still the authors retain that a carefully designed patch test can be considered as a valuable approach to investigate the quality of the interpolation scheme.

In what follows, we describe in some details a set of patch tests of a mixed finite element formulation for the thick plate theory.

- **Constant strain.** This is the original patch test and consist in checking that the discrete formulation is able to reproduce exactly all the constant strain states of the quantities involved in the functional of the specific problem. The satisfaction of this test guarantees consistency of the formulation and at the same time allows for a check of the computer code. Accordingly, for a thick plate problem, the following states must be reproduced:

  - *Constant bending curvature.* The plate is clamped along one edge and subjected to constant bending moment along the opposite edge; all the rotations in the direction orthogonal to the constant bending direction are kept fixed, to get a simple curvature problem.
  - *Constant shear strain.* The plate is clamped along one edge and subjected to constant shear force along the opposite edge; all the rotations are fixed in order to prevent bending.
  - *Constant twisting strain.* The plate is simply supported along two edges and subject to distributed constant edge twisting moments along the other two edges.

The test should be performed both on single element meshes and simple patches, with regular and non-regular element geometry, as shown in Figures 1-2. To investigate the *locking* in the limiting case of thin plates, it is important to run all the described test both for the cases of a thick and a thin plate. Moreover, between the thick and the thin case it is appropriate to keep the bending stiffness constant for the constant curvature test and the shear stiffness constant for the constant shear strain test [1], such that both the thin and the thick cases should return the same numerical responses.

- **Eigen-analysis of specific modes.** In this test, we perform the eigen-analysis of simple meshes which are allowed only specific deformation paths; accordingly we can study separately the bending, the shear and the twist eigen-modes. In particular, we suggest as appropriate to consider all the meshes presented in Figures 1-2, for both the thin and the thick case, with boundary conditions specified as on the three constant strain test.

  This analysis allows to evaluate how many modes are available to represent the bending and the shear response. To check and stress any tendency of the element to lock as well as ill-behaviors of the formulation in the limiting thin plate case, the bending stiffness should be kept constant for all the eigen-analysis.

- **Counts of the degrees of freedom.** This part of the mixed patch test consists in checking some simple algebraic inequalities involving the number of unknowns. For the particular formulation here discussed, the requirements are:

  $$n_\theta + n_w \geq n_s \quad , \quad n_s \geq n_w \tag{6.1}$$

  where n_w, n_θ and n_s stand for the number of degrees-of-freedom of $\hat{\mathbf{w}}$, $\hat{\boldsymbol{\theta}}$ and $\hat{\mathbf{S}}$ respectively. This test represent a necessary condition for the stability of the discrete problem, since they are necessary conditions for the solvability of the system 5.2.

  These counting relations should be satisfied for any generic finite element mesh and usually are checked for different *patches* (including

[1]To keep the bending stiffness constant the Young's modulus must be scaled proportional to $1/t^3$, while for keeping the shear stiffness constant it must be scaled by $1/t$.

both single elements and meshes with several elements, either with a maximum or a minimum number of essential boundary conditions).

- **Eigen-analysis of the stiffness matrix.** The eigenvalues of the stiffness matrix are computed and the presence of zero eigenvalues in excess of the number of rigid body modes is assessed, since it indicates *rank-deficiency* (or zero energy modes). Again the analysis is performed for the meshes shown in Figures 1-2, for the thick and thin case.

  The importance of this test is related to the fact that solving more general problems using rank-deficient elements can lead to instability in the solution and often results in non converging solutions (such as oscillations fluctuating around the exact solution) or occasionally in a singular global stiffness matrix. The presence of extra zero eigenvalues at a multi-element level must be considered as an index of possible ill-conditioned behavior and non-robustness of the formulation. If such singularity exists only for a single element, the issue is not so clear but still remain non desirable.

7 FINITE ELEMENT APPROXIMATION

We now present a new family of quadrilateral finite elements, developed within the thick plate theory discussed in Section 2.

7.1 A new family of thick plate finite elements

All the elements here described are of iso-parametric type, with four nodes. We use the usual bi-linear shape functions to map the parent domain in natural coordinates (ξ, η) to its real domain; accordingly the quadrilateral region occupied by each element may be expressed by

$$\mathbf{x} = \sum_{i=1}^{4} N^i \mathbf{x}^i$$

where $\mathbf{x} = \{x, y\}^T$ and $\mathbf{x}^i = \{x^i, y^i\}^T$ are the nodal coordinates [2]; N^i are the bi-linear shape function:

$$N^i = \frac{1}{4}\left(1 + \xi^i \xi\right)\left(1 + \eta^i \eta\right)$$

following for example the definition of Reference [9].

The elements have three external (global) displacement degrees-of-freedom at each vertex i: the transverse displacement $\hat{w}_i$ and the two components of the rotation along the x-y coordinate axes, $\hat{\theta}^i_x$ and $\hat{\theta}^i_y$, respectively. In addition, to improve the interpolation, they might have internal internal rotational degrees-of-freedom, associated with bubble functions.

The transverse displacement interpolation is taken as a simple linear function, enhanced by quadratic terms expressed in terms of the normal components of the nodal rotations for each side of the element:

$$w = \sum_{i=1}^{4} N^i \hat{w}^i - \sum_{i=1}^{4} N^i_{w\theta} L^i \left(\hat{\theta}^j_n - \hat{\theta}^i_n\right)$$

where $\hat{\theta}^j_n$ and $\hat{\theta}^i_n$ are the components of the rotations of nodes j and i in the direction normal to the i-j side, while L^i is the length of the side between nodes i and j (Figure 3). The $N^i_{w\theta}$ are appropriate shape functions of the form:

$$\mathbf{N}_{w\theta} = \left\{ \begin{array}{c} N^1_{w\theta} \\ N^2_{w\theta} \\ N^3_{w\theta} \\ N^4_{w\theta} \end{array} \right\} = \frac{1}{16} \left\{ \begin{array}{c} (1-\xi^2)(1-\eta) \\ (1+\xi)(1-\eta^2) \\ (1-\xi^2)(1+\eta) \\ (1-\xi)(1-\eta^2) \end{array} \right\}$$

The interpolation for the rotational fields is what distinguishes the three elements here presented. All the elements use at least a linear field, enriched progressively with internal modes associated with bubble functions; the different interpolation schemes adopted are concisely presented in the following table:

$$\begin{array}{lll} \text{Q4L0} & \Rightarrow & \boldsymbol{\theta} = \sum_{i=1}^4 N^i \hat{\boldsymbol{\theta}}^i \\ \text{Q4L1} & \Rightarrow & \boldsymbol{\theta} = \sum_{i=1}^4 N^i \hat{\boldsymbol{\theta}}^i + M \boldsymbol{\Delta} \hat{\boldsymbol{\theta}}^1 \\ \text{Q4L3} & \Rightarrow & \boldsymbol{\theta} = \sum_{i=1}^4 N^i \hat{\boldsymbol{\theta}}^i + M \left[\boldsymbol{\Delta} \hat{\boldsymbol{\theta}}^1 + \xi \boldsymbol{\Delta} \hat{\boldsymbol{\theta}}^2 + \eta \boldsymbol{\Delta} \hat{\boldsymbol{\theta}}^3 \right] \end{array}$$

[2] The indices i and j always range in $\{1, 2, 3, 4\}$.

with:

$$\hat{\boldsymbol{\theta}}^i = \left\{ \begin{array}{c} \hat{\theta}_x^i \\ \hat{\theta}_y^i \end{array} \right\} \quad , \quad \boldsymbol{\Delta}\hat{\boldsymbol{\theta}}^1 = \left\{ \begin{array}{c} \Delta\hat{\theta}_x^1 \\ \Delta\hat{\theta}_y^1 \end{array} \right\} \quad , \quad \boldsymbol{\Delta}\hat{\boldsymbol{\theta}}^2 = \left\{ \begin{array}{c} \Delta\hat{\theta}_x^2 \\ \Delta\hat{\theta}_y^2 \end{array} \right\} \quad , \quad \boldsymbol{\Delta}\hat{\boldsymbol{\theta}}^3 = \left\{ \begin{array}{c} \Delta\hat{\theta}_x^3 \\ \Delta\hat{\theta}_y^3 \end{array} \right\}$$

where $\hat{\boldsymbol{\theta}}^i$ $(i = 1, .., 4)$ are the nodal rotations, $\boldsymbol{\Delta\theta}^1, \boldsymbol{\Delta\theta}^2, \boldsymbol{\Delta\theta}^3$ are the internal rotational degrees of freedom, $M = (1-\xi^2)(1-\eta^2)$ is a bubble function. The last number in the element name indicates the number of bubble modes in the rotational field.

Finally, the shear interpolation is equal for all the three elements. In natural coordinates we choose:

$$\left\{ \begin{array}{c} S_\xi \\ S_\eta \end{array} \right\} = \left\{ \begin{array}{c} S^1 + \eta S^3 \\ S^2 + \xi S^4 \end{array} \right\}$$

where S^j $(j = 1, .., 4)$ are parameter local to each element. Accordingly to the transformation discussed in Reference [23], the interpolation field in the mapped element may be expressed as:

$$\mathbf{S} = \left\{ \begin{array}{c} S_x \\ S_y \end{array} \right\} = \left[\begin{array}{cccc} 1 & 0 & F_{11}^o \eta & F_{12}^o \xi \\ 0 & 1 & F_{21}^o \eta & F_{22}^o \xi \end{array} \right] \left\{ \begin{array}{c} S^1 \\ S^2 \\ S^3 \\ S^4 \end{array} \right\}$$

where:

$$F_{i1}^o = \frac{\partial x_i}{\partial \xi}|_{\xi=\eta=0} \quad , \quad F_{i2}^o = \frac{\partial x_i}{\partial \eta}|_{\xi=\eta=0}$$

The integration for the stiffness computation are performed numerically and we use respectively two, three and four integration points in each direction, respectively for the Q4L0, Q4L1, Q4L3 elements.

For the results reported in the next section, the finite element load is consistent with the transverse displacement interpolation.

8 NUMERICAL EXAMPLES

The performance of the family of finite elements previously discussed has been checked on all the patch tests discussed in Section 6 and on several standard numerical tests. The elements have been implemented into the Finite Element Analysis Program (FEAP) [34, 35] and this environment has been used for all the computations.

The solutions have always been compared with those obtained from other well performing elements available in literature. In particular we choose the T3L element [27] and the Q4L element [36], which are also based on a linked interpolation concept, the former being a triangular element; moreover, we report the results from the T1 element, described in References [9] and [11]. When available, analytical or series solutions are also reported.

The test problems are organized in the following order:

- Patch test: stability assessment
- Patch test: consistency assessment
- Square plate
- Circular plate
- Skew cantilever plate
- Simply supported skew plate

Only uniform loading is considered, since the transverse displacement for a concentrated load is infinite for a theory which includes the effects of shear deformation.

8.1 Patch test: stability assessment

The algebraic requirements of equation 6.1 have been checked on different meshes (including both single elements and meshes with several elements, either with a maximum or a minimum number of essential boundary conditions). For the count purpose we assume that one shear parameter is always shared between the side of two adjacent elements.

All the elements pass this test except Q4L0 in the 2×2 mesh with all the boundary fixed.

Since the constraint count is just a necessary condition for the stability of the formulation, an eigen-analysis on the stiffness matrix for patches of one or more elements (Figures 1-2) is performed, as described in section 6.

We consider a thick and a thin case, $L/h = 10$ and $L/h = 1000$ respectively, with $x = 2$. The presence of the correct number of zero eigen-values has been checked. All the elements proposed in the present work pass this test (Tables 1-4), while we recall that element Q4L does not, as described in Reference [36].

Recalling that we keep the bending stiffness constant while reducing the thickness (going from the thick plate to the thin one), it is extremely interesting to observe the number of growing eigenvalues, which are clearly those associated with the shear part of the stiffness: note that Q4L0, Q4L1, Q4L3 have respectively four, two and no growing eigenvalues. To really test the elements we consider also an extremely thin plate, $L/h = 100000$ (Table 5-6), and you may note that while the eigen-values for the regular mesh show no ill-condition, for the distorted case Q4L3 seems to lose the rigid body motion eigen-values and this is due to round-off during the static condensation of the internal parameters (rotational degrees of freedom associate with bubble modes and shear parameters).

8.2 Patch test: consistency assessment

To assess consistency the capacity of exactly reproducing constant strain states has been tested again on the meshes of Figures 1 and 2, for a thick and a thin case ($L/h = 10$ and $L/h = 1000$). To highlight pathologies in the limiting case of thin plates, the bending stiffness is kept constant during the constant curvature test, while the shear stiffness is kept constant during the constant shear strain test.

All the elements proposed in Section 6 pass the above consistency tests. Note however that T1 does not pass the test perfectly for the case of non-regular mesh; to show this, in Table 7 we report the results for the constant shear strain test with the ratio between the displacements of nodes b and c (Figure 1). The same problem can be retrieved if the non-regular mesh of Figure 2 is used.

We also perform the eigen-analysis of the meshes which may be vibrate only with specific modes; the idea is to study separately the bending, the shear and the twisted modes. In Table 8 we reported the eigen-values for the case of the shear modes only, where the bending stiffness is kept constant between the thin and the thick problems.

8.3 Square plate

A square plate is modeled using meshes of the type presented in Figure 4. Two simply supported boundary conditions are considered: *soft* and *hard*, discussed in References [9] and [34]. The results for a clamped plate are also presented.

The side length of the plate is $L = 1$ and both a thick ($L/h = 10, h = 0.1$) and a thin plate ($L/h = 1000, h = 0.001$) are considered. The material properties are:

$$E = 10.92 \quad , \quad \nu = 0.3$$

The numerical results are presented in Tables 9-14. The series solution for the thin plate applies to both the case of soft and hard support; the series solution for the thick plate (accounting for the shear deformation) is reported only for the case of hard boundary condition, since a solution for a thick soft simply supported boundary condition is more difficult to compute as the twist moments must vanish at each edge.

8.4 Circular plate

Also for the circular geometry (Figure 5) [3] two values of the thickness ($h = 0.1$ and $h = 1$) have been considered to simulate a thin and a thick plate. The radius R is set equal to 5.0, the load is $q = 1.0$ and the material properties are:

$$E = 10.92 \quad , \quad \nu = 0.3$$

The numerical results are presented in Tables 15-18, together with an analytical solution, which can be computed in closed form, both for the case of simply supported and clamped boundaries.

8.5 Skew cantilever plates

A skew cantilever plate clamped along the boundary 3-4 (Figure 6) is analyzed using three different values of the skew angle, β, between 20^o and 60^o; the 8x8 mesh with $\beta = 40^o$ is represented in Figure 7. The material properties

[3] The mesh is generated using three blocks of elements and the central nodes has coordinate $(2.1R, 2.1R)$, where R is the radius of the plate.

used are:

$$E = 10.92 \quad , \quad \nu = 0.3$$

with thickness $h = 4$, side length $L = 100$ and unit uniform load. The solution is expressed in term of displacement at points 1 and 2 (Figure 6) and is reported in Tables 19-21.

8.6 Simply supported skew plate

We consider a highly skewed plate ($\beta = 60^o$), simply supported along all boundaries. The plate has side length 100, the load is 1.0 and two different thickness are considered. The material properties are:

$$E = 10.92 \quad , \quad \nu = 0.3$$

The displacement and the two principal bending moments at the center of the plate are reported in Tables 22-23.

In addition, in Table 24 we perform a comparison of the element performances in terms of energy, as suggested in Reference [5]. The properties used are:

$$E = 3.0E7 \quad , \quad \nu = 0.3$$

with thickness $t = 0.01$, side length $L = 1$ and unit uniform load.

CLOSURE

In the present paper we present a new family of quadrilateral finite elements developed within the framework of a shear deformable plate theory. All the elements take advantages of the so-called *linked* interpolation, i.e. an explicit dependence of the transverse displacement on the discrete rotational field. The reasons which make convenient the use of this type of interpolation can be summarized as follow:

- with an appropriate choice of the $\mathbf{N}_{w\theta}$ shape functions we are able to obtain a constant shear strain along each side of the finite element,
- we guarantee a higher order interpolation for the transverse displacement than for the rotational field, as is required for the thin plate situation, when the latter are simply the derivative of the former,

- we have a transverse displacement interpolation with as few nodal parameter as possible, which is required for a satisfaction of the mixed patch test.

We performed a careful study of the element behaviors, based on an extensive set of mixed patch test. Moreover, the results for a wide group of standard numerical examples are presented, together with the results from three other elements available in literature. All the elements show proper rank, good interpolating capacity and no locking effects in the limiting case of thin plate. In particular, one of the element discussed, Q4L1, seems to be the most convenient in terms of computational costs versus performances.

References

[1] D.J. Allman, *A quadrilateral finite element including vertex rotations for plane elasticity analysis*, Intenational Journal for Numerical Methods in Engineering **26** (1988), 717–730.

[2] F. Auricchio and R.L. Taylor, *3-node triangular elements based on Reissner-Mindlin plate theory*, Report UCB/SEMM-91/04, Department of Civil Engineering, University of California at Berkeley, 1991, Copies available through NISEE. E-mail: nisee@cmsa.berkeley.edu.

[3] I. Babuska, *Error bounds for finite element methods*, Num. Math. **16** (1971), 322–333.

[4] ———, *The finite element method with lagrange multipliers*, Num. Math. **20** (1973), 179–192.

[5] I. Babuska and T. Scapolla, *Benchmark computation and performance evaluation for rhombic plate bending problem*, International Journal for Numerical Methods in Engineering **28** (1989), 155–179.

[6] G.P. Bazeley, Y.K. Cheung, B.M.Irons, and O.C.Zienkiewicz, *Triangular elements in bending - conforming and non-conforming solution*, Proc. Conf. on Matrix Methods in Structural Mechanics (Wright-Paterson Air Force Base, Ohio), 1965.

[7] F. Brezzi, *On the existence, uniqueness and approximation of saddle point problems arising from lagrange multipliers*, RAIRO **8** (1971), 129–151.

[8] A.E. Green and P.M. Naghdi, *On the derivation of shell theories by direct approach*, Journal of Applied Mechanics **41** (1974), 173–176.

[9] T.J.R. Hughes, *The finite element method*, Prentice Hall, 1987.

[10] T.J.R. Hughes and M. Cohen, *The heterosis finite element for plate bending*, Computer & Stuctures **9** (1978), 445–450.

[11] T.J.R. Hughes and T.E. Tezduyar, *Finite element based upon Mindlin plate theory with particular reference to the four node bilinear isoparametric element*, Journal of Applied Mechanics **48** (1981), 587–596.

[12] B.M. Irons, *Numerical integration applied to finite element methods*, Conf. on use of digital computers in structural engineering (University of Newcastle), 1966.

[13] B.M. Irons and A.Razzaque, *Experience with the patch test for convergence of finite element method*, Mathematical foundations of the finite element method (A.K. Aziz, ed.), Academic Press, 1972, pp. 557–587.

[14] R.D. Mindlin, *Influence of rotatory inertia and shear in flexural motion of isotropic, elastic plates*, Journal of Applied Mechanics **18** (1951), 31–38.

[15] P.M. Naghdi, *Finite deformation of elastic rods and shells*, Proc. IUTAM Symposium on Finite Elasticity (Bethlehem PA) (D.E. Carlson and R.T. Shield, eds.), 1982, pp. 47–103.

[16] O.C.Zienkiewicz and D.Lefebvre, *Three-field mixed approximation and the plate bending problem*, Comm. Appl. Numer. Meth. **3** (1987), 301–309.

[17] ———, *Mixed methods for F.E.M. and the patch test: some recent development*, Analyse Mathematique et Applications, Gauthier-Villars, 1988.

[18] O.C.Zienkiewicz, S.Qu, R.L.Taylor, and S.Nakazawa, *The patch test for mixed formulation*, International Journal for Numerical Methods in Engineering **23** (1986), 1873–1883.

[19] E.R. De Arantes Oliveira, *The patch test and the general convergence criteria of the finite element method*, International Journal Solids and Structures **13** (1977), 159–178.

[20] E. Reissner, *The effect of transverse shear deformation on the bending of elastic plates*, Journal of Applied Mechanics **12** (1945), 69–76.

[21] J.C. Simo and D.D. Fox, *On a stress resultant geometrically exact shell model. Part I: formulation and optimal parametrization*, Computer Methods in Applied Mechanics and Engineering (1988).

[22] J.C. Simo, D.D. Fox, and M.S. Rifai, *On a stress resultant geometrically exact shell model. Part II: the linear theory, computational aspects*, Computer Methods in Applied Mechanics and Engineering **73** (1989), 53–92.

[23] J.C. Simo and M.S. Rifai, *A class of mixed assumed strain methods and the method of incompatible modes*, International Journal for Numerical Methods in Engineering **29** (1990), 1595–1638.

[24] G. Strang and G.J. Fix, *An analysis of the finite element method*, Prentice Hall, 1973.

[25] R.L. Taylor, *Finite element analysis of linear shell problems*, MAFELAP 1987: the mathematics of finite elements and applications VI (J. Whiteman, ed.), Academic Press, 1987.

[26] R.L. Taylor and F. Auricchio, *Finite element analysis of linear shell problems.*

[27] ———, *Linked interpolation for Reissner-Mindlin plate elements: Part II: a simple triangle*, International Journal for Numerical Methods in Engineering **36** (1993), 3057–3066.

[28] R.L. Taylor and J.C.Simo, *Bending and membrane elements for analysis of thick and thin shells*, Proceedings of the NUMETA 85 Conference (G.N. Pande and J. Middleton, eds.), 1985, pp. 587–591.

[29] R.L. Taylor, J.C.Simo, O.C.Zienkiewicz, and C.H.Chan, *The patch test - a condition for assessing FEM convergence*, International Journal for Numerical Methods in Engineering **22** (1986), 39–62.

[30] B. Fraeijs De Veubeke, *Variational principle and the patch test*, International Journal for Numerical Methods in Engineering **8** (1974), 783–801.

[31] Z. Xu, *A simple and efficient triangular finite element for plate bending*, Acta Mechanica Sinica **2** (1986), 185–192.

[32] ———, *A thick-thin triangular plate element*, International Journal for Numerical Methods in Engineering **33** (1992), 963–973.

[33] Z. Xu, O.C. Zienkiewicz, and L.F. Zeng, *Linked interpolation for Reissner-Mindlin plate elements: Part III: an alternative quadrilateral*, International Journal for Numerical Methods in Engineering (1993), to appear.

[34] O.C. Zienkiewicz and R.L. Taylor, *The finite element method*, fourth ed., vol. I, McGraw Hill, New York, 1989.

[35] ———, *The finite element method*, fourth ed., vol. II, McGraw Hill, New York, 1991.

[36] O.C. Zienkiewicz, Z. Xu, L.F. Zeng, A. Samuelsson, and N.E. Wiberg, *Linked interpolation for Reissner-Mindlin plate elements: Part I: a simple quadrilateral*, International Journal for Numerical Methods in Engineering **36** (1993), 3043–3056.

Q4L0	1.0077E+02	1.0077E+02	3.2149E+01	2.9167E+01	1.3000E+00	7.0000E-01
	4.0639E-01	4.0639E-01	5.0805E-02	-4.9420E-15	3.8067E-15	-2.2559E-15
Q4L1	3.2149E+01	2.9167E+01	5.8593E+00	5.8593E+00	1.3000E+00	7.0000E-01
	2.9671E-01	2.9671E-01	5.0805E-02	8.2070E-16	-4.3691E-16	2.5602E-16
Q4L3	5.8593E+00	5.8593E+00	4.6029E+00	2.6200E+00	1.3000E+00	7.0000E-01
	2.9671E-01	2.9671E-01	4.4467E-02	1.0747E-15	4.9788E-16	-1.5759E-16
T1	9.1000E+01	9.1000E+01	3.2149E+01	2.9167E+01	1.3000E+00	7.0000E-01
	4.5000E-01	4.5000E-01	5.0805E-02	8.2750E-15	-5.3812E-15	3.3604E-16

Table 1: Eigenvalues thick regular mesh ($L/t = 10$)

Q4L0	1.1344E+02	1.0885E+02	3.4813E+01	3.2055E+01	1.3317E+00	6.9367E-01
	4.3973E-01	3.7457E-01	4.6793E-02	9.1290E-15	1.3183E-15	-3.8474E-16
Q4L1	3.4884E+01	3.2274E+01	6.4926E+00	5.4018E+00	1.3315E+00	6.9107E-01
	3.1996E-01	2.7546E-01	4.6754E-02	8.5528E-16	-5.7383E-16	4.3584E-16
Q4L3	6.5052E+00	5.4639E+00	4.6317E+00	2.6741E+00	1.3302E+00	6.8876E-01
	3.1919E-01	2.7517E-01	4.0814E-02	7.8272E-16	-6.5417E-16	-4.3370E-16
T1	1.0118E+02	9.9528E+01	3.5361E+01	3.2498E+01	1.3282E+00	6.8962E-01
	4.8377E-01	4.2317E-01	4.6886E-02	3.4031E-15	2.4513E-15	-2.0133E-15

Table 2: Eigenvalues thick irregular mesh ($L/t = 10$)

Q4L0	1.0072E+06	1.0072E+06	3.1500E+05	2.9167E+05	1.3000E+00	7.0000E-01
	4.0656E-01	4.0656E-01	5.1852E-02	8.9187E-11	-1.7118E-11	-2.6383E-12
Q4L1	3.1500E+05	2.9167E+05	6.1808E+00	6.1808E+00	1.3000E+00	7.0000E-01
	2.9690E-01	2.9690E-01	5.1852E-02	-1.5015E-11	-4.0098E-12	1.7169E-12
Q4L3	6.1808E+00	6.1808E+00	5.1675E+00	2.8785E+00	1.3000E+00	7.0000E-01
	2.9690E-01	2.9690E-01	4.5282E-02	2.7542E-12	-1.9937E-12	-1.2406E-12
T1	9.1000E+05	9.1000E+05	3.1500E+05	2.9167E+05	1.3000E+00	7.0000E-01
	4.5000E-01	4.5000E-01	5.1852E-02	-4.4830E-11	-2.2291E-11	3.7136E-12

Table 3: Eigenvalues thin regular mesh ($L/t = 1000$)

Q4L0	1.1339E+06	1.0881E+06	3.4174E+05	3.2031E+05	1.3319E+00	6.9382E-01
	4.3993E-01	3.7473E-01	4.7686E-02	-9.0690E-11	1.2309E-11	5.3036E-12
Q4L1	3.4234E+05	3.2224E+05	6.8437E+00	5.6614E+00	1.3317E+00	6.9123E-01
	3.2015E-01	2.7562E-01	4.7645E-02	-2.2938E-11	5.5739E-12	-2.7524E-12
Q4L3	6.8572E+00	5.7296E+00	5.1477E+00	2.9142E+00	1.3304E+00	6.8902E-01
	3.1938E-01	2.7534E-01	4.1503E-02	4.3076E-10	-4.1579E-10	1.5338E-10
T1	1.0117E+06	9.9527E+05	3.4712E+05	3.2484E+05	1.3284E+00	6.8979E-01
	4.8383E-01	4.2318E-01	4.7761E-02	9.9054E-11	4.5190E-12	3.5108E-12

Table 4: Eigenvalues thin irregular mesh ($L/t = 1000$)

Q4L0	1.0072E+10	1.0072E+10	3.1500E+09	2.9167E+09	1.3000E+00	7.0000E-01
	4.0656E-01	4.0656E-01	5.1852E-02	-9.6140E-07	2.7706E-07	-7.3916E-08
Q4L1	3.1500E+09	2.9167E+09	6.1808E+00	6.1808E+00	1.3000E+00	7.0000E-01
	2.9690E-01	2.9690E-01	5.1852E-02	-1.1430E-07	4.9166E-08	1.1797E-08
Q4L3	6.1808E+00	6.1808E+00	5.1676E+00	2.8786E+00	1.3000E+00	7.0000E-01
	2.9690E-01	2.9690E-01	4.5282E-02	8.3655E-08	4.4954E-08	8.8698E-09
T1	9.1000E+09	9.1000E+09	3.1500E+09	2.9167E+09	1.3000E+00	7.0000E-01
	4.5000E-01	4.5000E-01	5.1852E-02	-1.4452E-07	1.4444E-07	1.1585E-07

Table 5: Eigenvalues extremely-thin regular mesh ($L/t = 100000$)

Q4L0	1.1339E+10	1.0881E+10	3.4173E+09	3.2031E+09	1.3319E+00	6.9382E-01
	4.3993E-01	3.7473E-01	4.7686E-02	-7.1913E-08	-5.9541E-08	4.9550E-08
Q4L1	3.4234E+09	3.2224E+09	6.8437E+00	5.6615E+00	1.3317E+00	6.9123E-01
	3.2015E-01	2.7562E-01	4.7645E-02	-2.3181E-07	4.0241E-08	7.0141E-10
Q4L3	8.2814E+00	7.0049E+00	3.7847E+00	1.7357E+00	1.2235E+00	-1.1484E+00
	7.2832E-01	4.2503E-01	-9.8894E-02	7.2956E-02	-2.5870E-02	7.1905E-03
T1	1.0117E+10	9.9527E+09	3.4712E+09	3.2484E+09	1.3284E+00	6.8979E-01
	4.8383E-01	4.2318E-01	4.7761E-02	6.3630E-07	-1.4301E-07	-7.5890E-08

Table 6: Eigenvalues extremely-thin irregular mesh ($L/t = 100000$)

		Square		Non-square		
		w_b	w_c	w_b	w_c	w_b/w_c
Q4L0	thin	2.85714E-01	2.85714E-01	2.85714E-01	3.42857E-01	1.200000
	thick	2.85714E-01	2.85714E-01	2.85714E-01	3.42857E-01	1.200000
Q4L1	thin	2.85714E-01	2.85714E-01	2.85714E-01	3.42857E-01	1.200000
	thick	2.85714E-01	2.85714E-01	2.85714E-01	3.42857E-01	1.200000
Q4L3	thin	2.85714E-01	2.85714E-01	2.85714E-01	3.42857E-01	1.200000
	thick	2.85714E-01	2.85714E-01	2.85714E-01	3.42857E-01	1.200000
T1	thin	2.85714E-01	2.85714E-01	2.76524E-01	3.53237E-01	1.277418
	thick	2.85714E-01	2.85714E-01	2.76524E-01	3.53237E-01	1.277418

Table 7: Patch test for constant shear: single element test. The shear stiffness is kept constant (i.e $D = 10.92/t$)

		Square		Non-square	
Q4L0	thin	0.17500100D+05	0.29166767D+05	0.15646963D+05	0.31387132D+05
	thick	0.18500000D+01	0.30166667D+01	0.16646863D+01	0.32387032D+01
Q4L1	thin	0.19719946D+00	0.11666864D+05	0.39709610D+01	0.11689361D+05
	thick	0.19208532D+00	0.13587520D+01	0.17373139D+00	0.13688255D+01
Q4L3	thin	0.19719946D+00	0.36433992D+00	0.17568047D+00	0.36269779D+00
	thick	0.19208532D+00	0.33828310D+00	0.17216654D+00	0.33892319D+00
T1	thin	0.17500100D+05	0.29166767D+05	0.15429836D+05	0.32376907D+05
	thick	0.18500000D+01	0.30166667D+01	0.16429736D+01	0.33376807D+01

Table 8: Patch test for constant shear: single element eigen-analysis. The bending stiffness is kept constant (i.e. $D = 10.92/t^3$)

	Q4L0		Q4L1		Q4L3	
Mesh	w / $(\frac{qL^4}{100D})$	M / $(\frac{qL^2}{100})$	w / $(\frac{qL^4}{100D})$	M / $(\frac{qL^2}{100})$	w / $(\frac{qL^4}{100D})$	M / $(\frac{qL^2}{100})$
2 x 2	0.437475	4.51841	0.453375	4.51285	0.460162	4.54977
4 x 4	0.449288	4.91023	0.454985	4.92130	0.456143	4.93074
8 x 8	0.456865	5.03404	0.458668	5.04011	0.458810	5.04132
16 x 16	0.460264	5.07833	0.460760	5.08024	0.460771	5.08034
32 x 32	0.461316	5.09121	0.461444	5.09172	0.461444	5.09172
T3L	0.460839	5.09002	0.460839	5.09002	0.460839	5.09002
Q4L	0.461793	5.09626	0.461793	5.09626	0.461793	5.09626
T1	0.461267	5.90037	0.461267	5.90037	0.461267	5.90037

Table 9: Simply supported square plate $L/h = 10$, $h = 0.1$, soft boundary: displacements and moments at the center.

	Q4L0		Q4L1		Q4L3	
Mesh	w / $(\frac{qL^4}{100D})$	M / $(\frac{qL^2}{100})$	w / $(\frac{qL^4}{100D})$	M / $(\frac{qL^2}{100})$	w / $(\frac{qL^4}{100D})$	M / $(\frac{qL^2}{100})$
2 x 2	0.367595	3.66614	0.410641	4.47850	0.422938	4.41903
4 x 4	0.371920	4.03808	0.407200	4.70696	0.412569	4.73452
8 x 8	0.404151	4.76176	0.406506	4.76741	0.409106	4.78732
16 x 16	0.406064	4.78309	0.406395	4.78330	0.407642	4.79448
32 x 32	0.406221	4.78744	0.406397	4.78840	0.406954	4.79334
T3L	0.406408	4.78978	0.406408	4.78978	0.406408	4.78978
Q4L	0.408609	4.80917	0.408609	4.80917	0.408609	4.80917
T1	0.406230	4.78703	0.406230	4.78703	0.406230	4.78703
Ser.thin	0.406235	4.78863	0.406235	4.78863	0.406235	4.78863

Table 10: Simply supported square plate $L/h = 1000$, $h = 0.001$, soft boundary: displacements and moments at the center.

	Q4L0		Q4L1		Q4L3	
Mesh	w / ($\frac{qL^4}{100D}$)	M / ($\frac{qL^2}{100}$)	w / ($\frac{qL^4}{100D}$)	M / ($\frac{qL^2}{100}$)	w / ($\frac{qL^4}{100D}$)	M / ($\frac{qL^2}{100}$)
2 x 2	0.415492	4.41062	0.426066	4.35708	0.426243	4.35309
4 x 4	0.424718	4.69703	0.427176	4.68143	0.427199	4.68134
8 x 8	0.426655	4.76582	0.427269	4.76185	0.427270	4.76185
16 x 16	0.427128	4.78294	0.427281	4.78194	0.427281	4.78194
32 x 32	0.427245	4.78721	0.427283	4.78696	0.427283	4.78696
T3L	0.427177	4.78915	0.427177	4.78915	0.427177	4.78915
Q4L	0.427288	4.78841	0.427288	4.78841	0.427288	4.78841
T1	0.427256	4.78681	0.427256	4.78681	0.427256	4.78681
Ser.thick	0.427284	4.78863	0.427284	4.78863	0.427284	4.78863

Table 11: Simply supported square plate $L/h = 10$, $h = 0.1$, hard boundary: displacements and moments at the center.

	Q4L0		Q4L1		Q4L3	
Mesh	w / ($\frac{qL^4}{100D}$)	M / ($\frac{qL^2}{100}$)	w / ($\frac{qL^4}{100D}$)	M / ($\frac{qL^2}{100}$)	w / ($\frac{qL^4}{100D}$)	M / ($\frac{qL^2}{100}$)
2 x 2	0.014215	0.16490	0.405589	4.31045	0.403673	4.34455
4 x 4	0.295853	3.64487	0.406215	4.67080	0.405862	4.68141
8 x 8	0.403722	4.76207	0.406221	4.76047	0.406157	4.76186
16 x 16	0.406037	4.78292	0.406223	4.78209	0.406218	4.78194
32 x 32	0.406194	4.78721	0.406233	4.78697	0.406233	4.78696
T3L	0.406150	4.78747	0.406150	4.78747	0.406150	4.78747
Q4L	0.406232	4.78841	0.406232	4.78841	0.406232	4.78841
T1	0.406205	4.78681	0.406205	4.78681	0.406205	4.78681
Ser.thin	0.406235	4.78863	0.406235	4.78863	0.406235	4.78863
Ser.thick	0.406237	4.78863	0.406237	4.78863	0.406237	4.78863

Table 12: Simply supported square plate $L/h = 1000$, $h = 0.001$, hard boundary: displacements and moments at the center.

	Q4L0		Q4L1		Q4L3	
Mesh	w / ($\frac{qL^4}{100D}$)	M / ($\frac{qL^2}{100}$)	w / ($\frac{qL^4}{100D}$)	M / ($\frac{qL^2}{100}$)	w / ($\frac{qL^4}{100D}$)	M / ($\frac{qL^2}{100}$)
2 x 2	0.120869	1.83728	0.141112	1.81582	0.142038	1.81129
4 x 4	0.143734	2.20661	0.148518	2.19685	0.148574	2.19683
8 x 8	0.148768	2.29139	0.149969	2.28896	0.149974	2.28898
16 x 16	0.150036	2.31280	0.150337	2.31220	0.150337	2.31220
32 x 32	0.150356	2.31819	0.150431	2.31804	0.150431	2.31804
T3L	0.150382	2.31734	0.150382	2.31734	0.150382	2.31734
Q4L	0.150442	2.31954	0.150442	2.31954	0.150442	2.31954
T1	0.150436	2.31906	0.150436	2.31906	0.150436	2.31906
Ser.thick	0.1499	2.31	0.1499	2.31	0.1499	2.31

Table 13: Clamped square plate $L/h = 10$, $h = 0.1$: displacements and moments at the center.

	Q4L0		Q4L1		Q4L3	
Mesh	w / ($\frac{qL^4}{100D}$)	M / ($\frac{qL^2}{100}$)	w / ($\frac{qL^4}{100D}$)	M / ($\frac{qL^2}{100}$)	w / ($\frac{qL^4}{100D}$)	M / ($\frac{qL^2}{100}$)
2 x 2	0.170639	3.24026	0.105259	1.82404	0.114593	1.73130
4 x 4	0.105329	2.66584	0.120794	2.16255	0.123603	2.16287
8 x 8	0.095705	1.98067	0.125263	2.25739	0.125839	2.25898
16 x 16	0.124064	2.26452	0.126319	2.28233	0.126369	2.28271
32 x 32	0.126341	2.28799	0.126491	2.28855	0.126495	2.28858
T3L	0.126429	2.28798	0.126429	2.28798	0.126429	2.28798
Q4L	0.126496	2.29003	0.126496	2.29003	0.126496	2.29003
T1	0.126511	2.28974	0.126511	2.28974	0.126511	2.28974
Ser.thin	0.1260	2.31	0.1260	2.31	0.1260	2.31
Ser.thick	0.1262	2.31	0.1262	2.31	0.1262	2.31

Table 14: Clamped square plate $L/h = 10$, $h = 0.1$: displacements and moments at the center.

	Q4L0		Q4L1		Q4L3	
Mesh	w	M	w	M	w	M
1	41.3303	4.87119	42.1964	4.80443	42.2268	4.80156
2	41.4817	5.08801	41.7599	5.06826	41.7631	5.06807
4	41.5669	5.13909	41.6406	5.13370	41.6408	5.13369
8	41.5911	5.15189	41.6098	5.15051	41.6098	5.15051
16	41.5973	5.15515	41.6020	5.15480	41.6020	5.15480
T3L	41.5971	5.15445	41.5971	5.15445	41.5971	5.15445
Q4L	41.6021	5.15479	41.6021	5.15479	41.6021	5.15479
T1	41.5864	5.15398	41.5864	5.15398	41.5864	5.15398
Ex.sol.	41.5994	5.1563	41.5994	5.1563	41.5994	5.1563

Table 15: Simply supported circular plate $R/h = 5$, $h = 1$: displacements and moments at the center.

	Q4L0		Q4L1		Q4L3	
Mesh	w	M	w	M	w	M
1	39621.4	4.85234	40577.1	4.81943	40596.4	4.80020
2	39714.8	5.05350	40026.6	5.07216	40028.6	5.06636
4	39805.8	5.13734	39881.4	5.13376	39881.5	5.13343
8	39825.3	5.15181	39844.1	5.15048	39844.1	5.15047
16	39830.0	5.15514	39834.7	5.15479	39834.7	5.15479
T3L	39828.7	5.15448	39828.7	5.15448	39828.7	5.15448
Q4L	39834.7	5.15479	39834.7	5.15479	39834.7	5.15479
T1	39819.0	5.15398	39819.0	5.15398	39819.0	5.15398
Ex.sol.	39831.5	5.1563	39831.5	5.1563	39831.5	5.1563

Table 16: Simply supported circular plate $R/h = 50$, $h = 0.1$: displacements and moments at the center.

	Q4L0		Q4L1		Q4L3	
Mesh	w	M	w	M	w	M
1	8.19394	1.42709	9.05855	1.36193	9.09004	1.35689
2	10.6597	1.88271	10.9378	1.86286	10.9410	1.86264
4	11.3256	1.99401	11.3993	1.98860	11.3995	1.98860
8	11.4947	2.02187	11.5134	2.02049	11.5134	2.02049
16	11.5372	2.02889	11.5419	2.02854	11.5419	2.02854
T3L	11.5207	2.02665	11.5207	2.02665	11.5207	2.02665
Q4L	11.5419	2.02854	11.5419	2.02854	11.5419	2.02854
T1	11.5488	2.03007	11.5488	2.03007	11.5488	2.03007
Ex.sol.	11.5513	2.0313	11.5513	2.0313	11.5513	2.0313

Table 17: Clamped circular plate $R/h = 5$, $h = 1$: displacements and moments at the center.

	Q4L0		Q4L1		Q4L3	
Mesh	w	M	w	M	w	M
1	6482.28	1.40553	7455.06	1.37082	7459.88	1.35520
2	8892.34	1.84809	9206.67	1.86743	9206.64	1.86100
4	9564.48	1.99227	9640.09	1.98868	9640.21	1.98834
8	9728.96	2.02179	9747.72	2.02046	9747.74	2.02045
16	9769.85	2.02888	9774.55	2.02854	9774.55	2.02854
T3L	9753.53	2.02667	9753.53	2.02667	9753.53	2.02667
Q4L	9774.55	2.02854	9774.55	2.02854	9774.55	2.02854
T1	9781.39	2.03007	9781.39	2.03007	9781.39	2.03007
Ex.sol.	9783.48	2.0313	9783.48	2.0313	9783.48	2.0313

Table 18: Clamped circular plate $R/h = 50$, $h = 0.1$: displacements and moments at the center.

	Q4L0		Q4L1		Q4L3	
Mesh	w_1 (x $\frac{Et^3}{qL^4}$)	w_2 (x $\frac{Et^3}{qL^4}$)	w_1 (x $\frac{Et^3}{qL^4}$)	w_2 (x $\frac{Et^3}{qL^4}$)	w_1 (x $\frac{Et^3}{qL^4}$)	w_2 (x $\frac{Et^3}{qL^4}$)
2 x 2	1.14643	0.93056	1.26594	0.97725	1.29491	0.98087
4 x 4	1.35205	1.00747	1.38267	1.02304	1.38749	1.02658
8 x 8	1.41224	1.03358	1.41728	1.03839	1.41807	1.03939
16 x 16	1.42502	1.04109	1.42666	1.04272	1.42686	1.04291
32 x 32	1.42930	1.04363	1.42993	1.04416	1.42997	1.04419
T3L	1.42892	1.04384	1.42892	1.04384	1.42892	1.04384
Q4L	1.43091	1.04484	1.43091	1.04484	1.43091	1.04484
T1	1.43003	1.04376	1.43003	1.04376	1.43003	1.04376

Table 19: Skew cantilever plate with $\beta = 20^o$: displacements at point 1 and point 2.

	Q4L0		Q4L1		Q4L3	
Mesh	w_1 (x $\frac{Et^3}{qL^4}$)	w_2 (x $\frac{Et^3}{qL^4}$)	w_1 (x $\frac{Et^3}{qL^4}$)	w_2 (x $\frac{Et^3}{qL^4}$)	w_1 (x $\frac{Et^3}{qL^4}$)	w_2 (x $\frac{Et^3}{qL^4}$)
2 x 2	0.78142	0.436628	0.92707	0.462879	0.96089	0.462620
4 x 4	1.03700	0.508903	1.08247	0.518871	1.08861	0.518886
8 x 8	1.14291	0.534552	1.15095	0.537510	1.15155	0.537747
16 x 16	1.17212	0.542788	1.17523	0.544236	1.17537	0.544351
32 x 32	1.18332	0.546431	1.18513	0.547204	1.18516	0.547226
T3L	1.18401	0.547079	1.18401	0.547079	1.18401	0.547079
Q4L	1.18685	0.548103	1.18685	0.548103	1.18685	0.548103
T1	1.18482	0.546408	1.18482	0.546408	1.18482	0.546408

Table 20: Skew cantilever plate with $\beta = 40^o$: displacements at point 1 and point 2

	Q4L0		Q4L1		Q4L3	
Mesh	w_1 (x $\frac{Et^3}{qL^4}$)	w_2 (x $\frac{Et^3}{qL^4}$)	w_1 (x $\frac{Et^3}{qL^4}$)	w_2 (x $\frac{Et^3}{qL^4}$)	w_1 (x $\frac{Et^3}{qL^4}$)	w_2 (x $\frac{Et^3}{qL^4}$)
2 x 2	0.416628	0.102638	0.594765	0.103799	0.617981	0.101386
4 x 4	0.627058	0.128497	0.706588	0.130982	0.713873	0.130738
8 x 8	0.762912	0.143078	0.793401	0.146167	0.794249	0.146099
16 x 16	0.818908	0.150998	0.832221	0.153292	0.832321	0.153297
32 x 32	0.843262	0.155250	0.850080	0.156835	0.850096	0.156838
T3L	0.850237	0.157198	0.850237	0.157198	0.850237	0.157198
Q4L	0.851822	0.157164	0.851822	0.157164	0.851822	0.157164
T1	0.845001	0.155380	0.845001	0.155380	0.845001	0.155380

Table 21: Skew cantilever plate with $\beta = 60°$: displacements at point 1 and point 2.

	Q4L0			Q4L1			Q4L3		
Mesh	$\frac{w}{\frac{qL^4}{100D}}$	$\frac{M_1}{\frac{qL^2}{100}}$	$\frac{M_2}{\frac{qL^2}{100}}$	$\frac{w}{\frac{qL^4}{100D}}$	$\frac{M_1}{\frac{qL^2}{100}}$	$\frac{M_2}{\frac{qL^2}{100}}$	$\frac{w}{\frac{qL^4}{100D}}$	$\frac{M_1}{\frac{qL^2}{100}}$	$\frac{M_2}{\frac{qL^2}{100}}$
2 x 2	0.227448	34.6260	9.52345	0.516197	8.71856	-6.98057	0.563523	1.18538	0.62440
4 x 4	0.253486	6.37392	1.96260	0.415295	4.61806	0.48784	0.431559	1.82111	0.89319
8 x 8	0.356071	2.06756	1.03514	0.404688	2.08695	1.16959	0.420489	1.91164	1.06425
16 x 16	0.393561	1.88090	1.05898	0.414588	1.92960	1.11344	0.418855	1.93078	1.10869
32 x 32	0.409510	1.90980	1.09094	0.419246	1.93671	1.11974	0.419989	1.93854	1.12175
T3L	0.419586	1.93657	1.12122	0.419586	1.93657	1.12122	0.419586	1.93657	1.12122
Q4L	0.426951	1.96183	1.14877	0.426951	1.96183	1.14877	0.426951	1.96183	1.14877
T1	0.403831	1.88974	1.07009	0.403831	1.88974	1.07009	0.403831	1.88974	1.07009

Table 22: Simply supported skew plate $L/h = 100$, $h = 1$, soft boundary: displacements and moments at the center.

	Q4L0			Q4L1			Q4L3		
Mesh	$\frac{w}{\frac{qL^4}{100D}}$	$\frac{M_1}{\frac{qL^2}{100}}$	$\frac{M_2}{\frac{qL^2}{100}}$	$\frac{w}{\frac{qL^4}{100D}}$	$\frac{M_1}{\frac{qL^2}{100}}$	$\frac{M_2}{\frac{qL^2}{100}}$	$\frac{w}{\frac{qL^4}{100D}}$	$\frac{M_1}{\frac{qL^2}{100}}$	$\frac{M_2}{\frac{qL^2}{100}}$
2 x 2	0.167484	42.3622	12.8100	0.514182	8.74371	-6.90521	0.562471	1.18545	0.62348
4 x 4	0.143751	2.74687	0.92239	0.412490	4.76668	0.28582	0.430168	1.81880	0.89235
8 x 8	0.227808	1.44158	0.63561	0.354657	2.01223	1.06249	0.418027	1.90693	1.06332
16 x 16	0.324388	1.66299	0.82846	0.358479	1.78555	1.00688	0.413714	1.92057	1.10435
32 x 32	0.365821	1.78218	0.93491	0.382498	1.83752	1.01352	0.412125	1.91715	1.09843
T3L	0.412734	1.91781	1.09998	0.412734	1.91781	1.09998	0.412734	1.91781	1.09998
Q4L	0.423520	1.95282	1.14021	0.423520	1.95282	1.14021	0.423520	1.95282	1.14021
T1	0.361559	1.76889	0.91530	0.361559	1.76889	0.91530	0.361559	1.76889	0.91530

Table 23: Simply supported skew plate $L/h = 1000$, $h = 0.1$, soft boundary: displacements and moments at the center.

	Energy				
Mesh	Q4L0	Q4L1	Q4L3	T3L	Q4L
2 x 2	0.186062	0.361146	0.470719	0.383241	0.285103
4 x 4	0.179283	0.254242	0.272841	0.267398	0.256943
8 x 8	0.228214	0.250221	0.262314	0.261721	0.261289
16 x 16	0.247832	0.259143	0.261949	0.262122	0.262455
32 x 32	0.256664	0.262193	0.262669	0.262921	0.262708
Ref. [5]	0.265868	0.265868	0.265868	0.265868	0.265868

Table 24: Simply supported skew plate $L/h = 100$, $h = 1$, soft boundary: displacements and moments at the center.

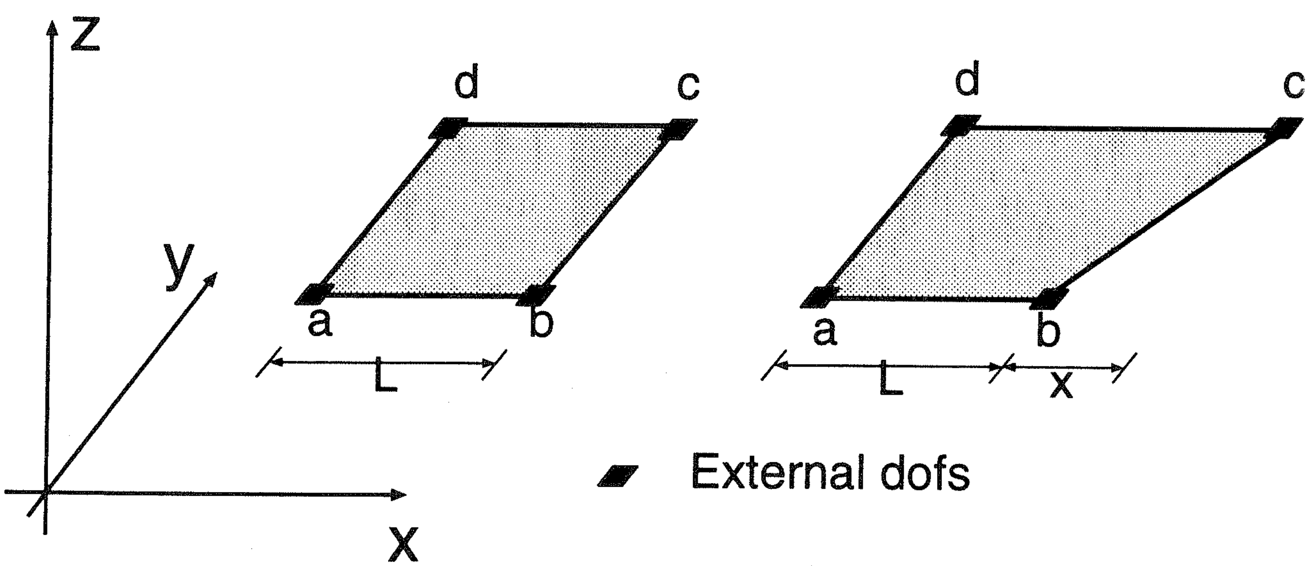

Figure 1: Single element meshes for patch test. Regular and non-regular mesh.

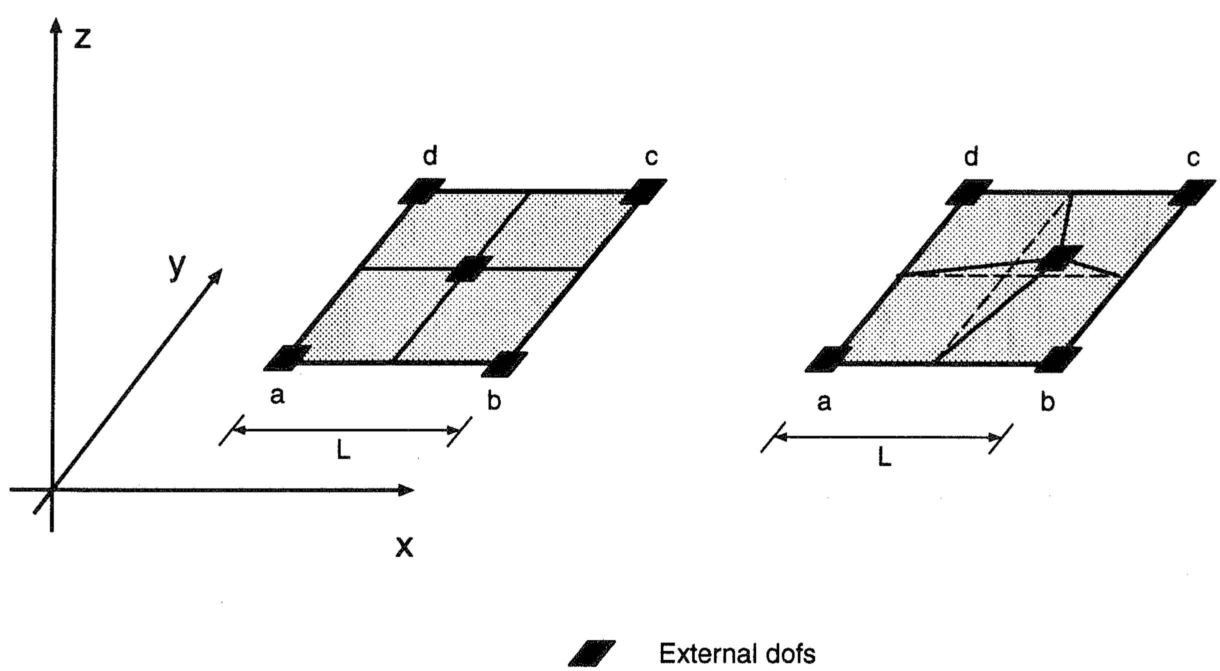

Figure 2: Multi element meshes for patch test. Regular and non-regular mesh.

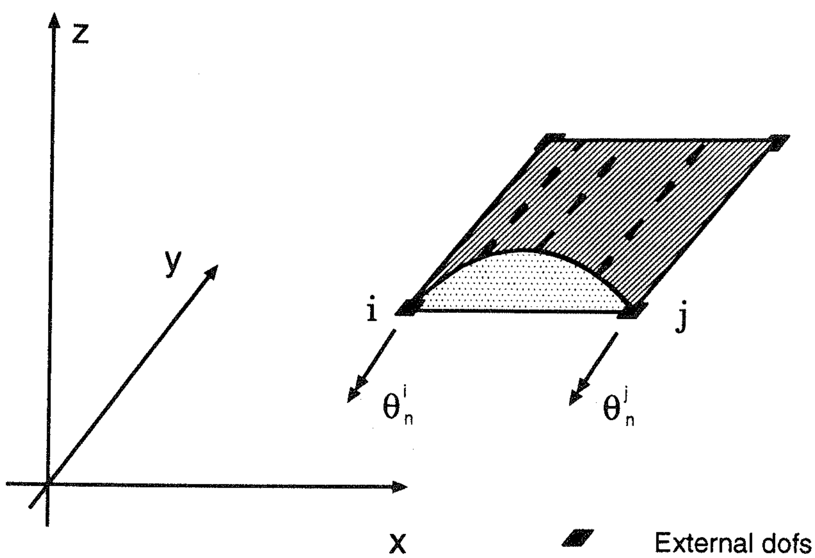

Figure 3: Design of the linked shape function $\mathbf{N}_{w\theta}$ for the a-b side.

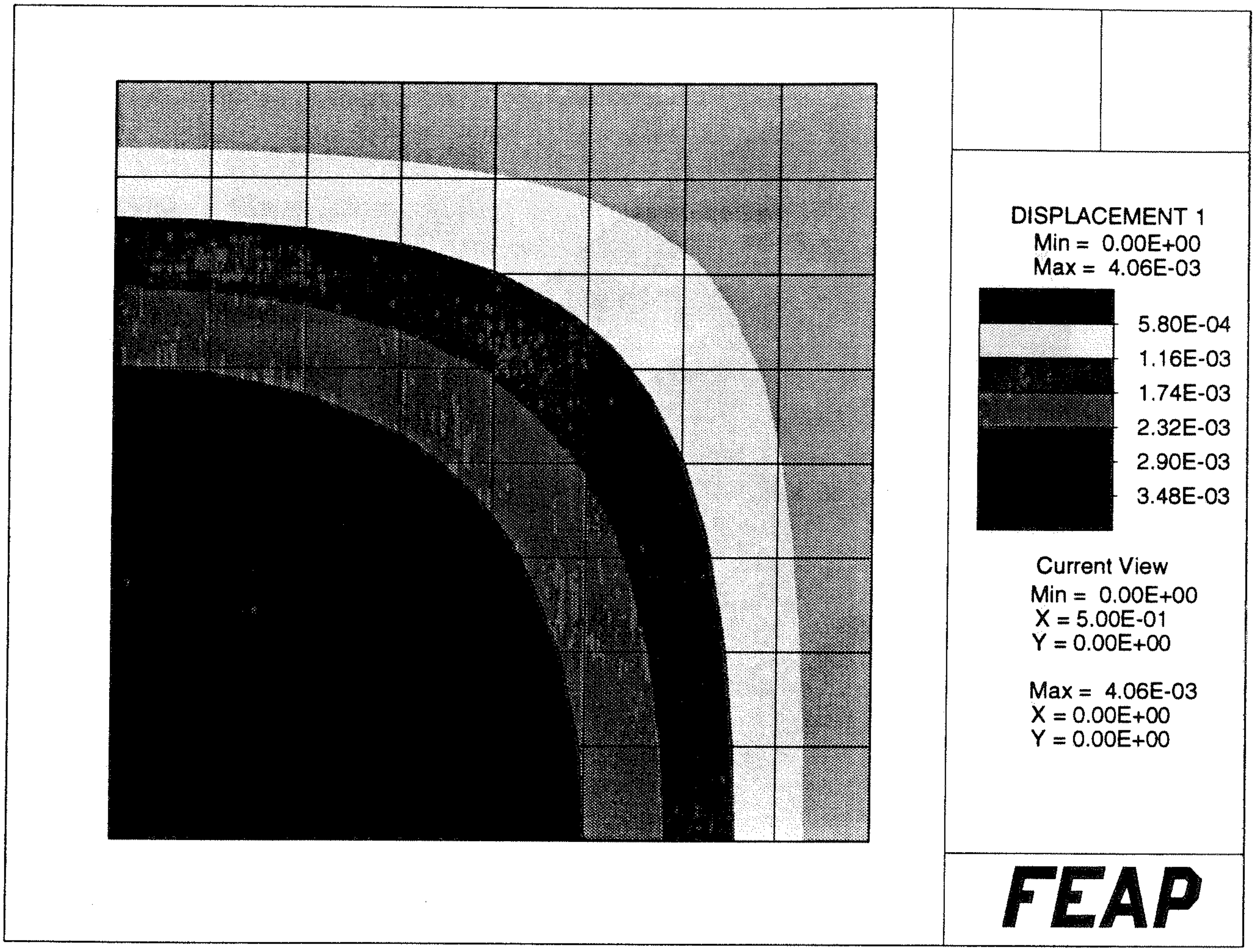

Figure 4: Typical mesh for square plate (8×8 elements). The contour of the vertical displacement (Q4L1) is also reported.

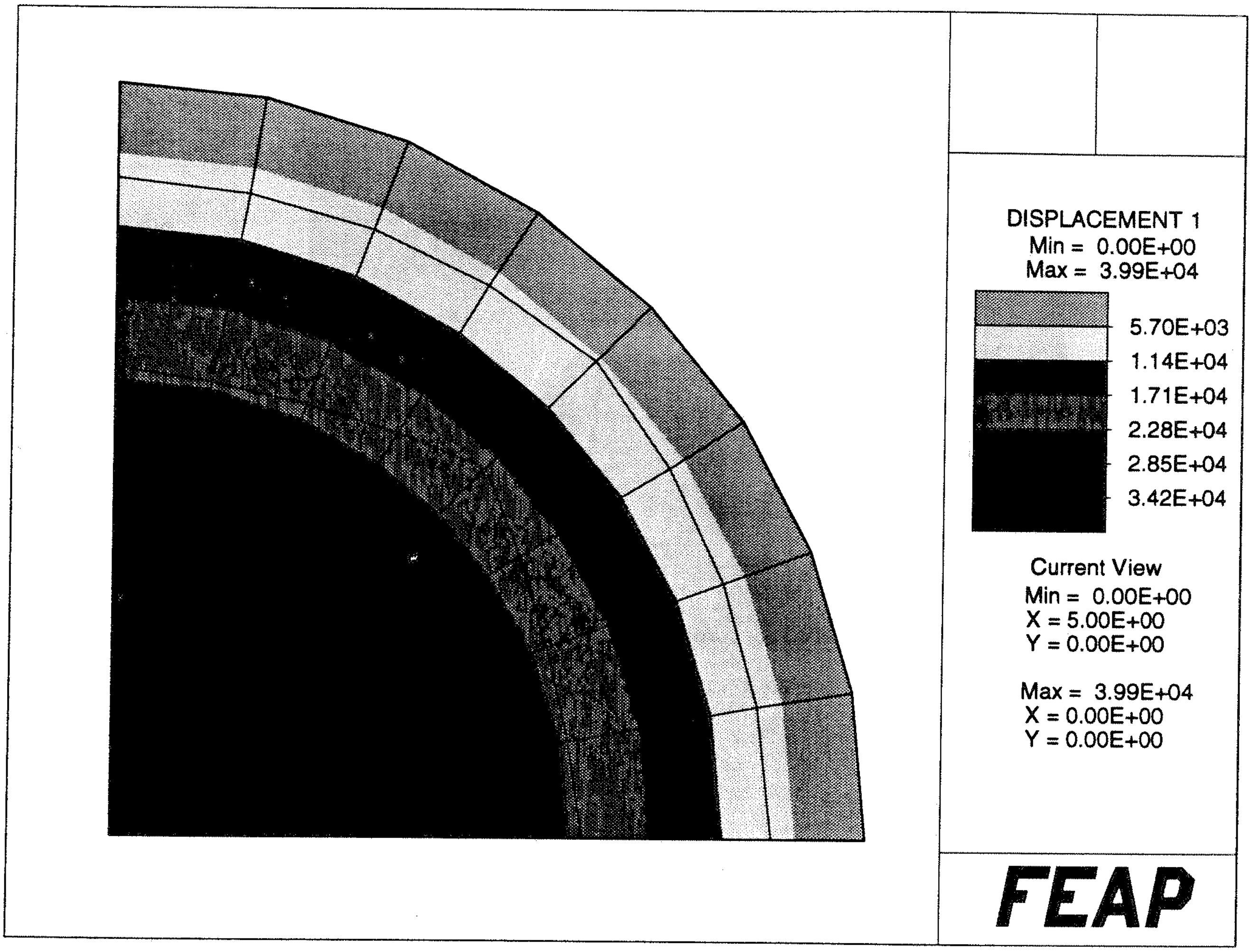

Figure 5: Typical mesh for circular plate (48 elements). The contour of the vertical displacement (Q4L1) is also reported.

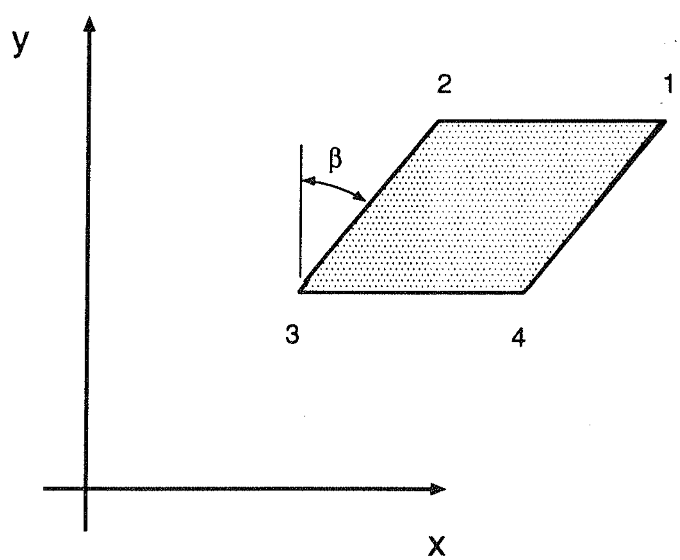

Figure 6: Geometry of the skew cantilever plate.

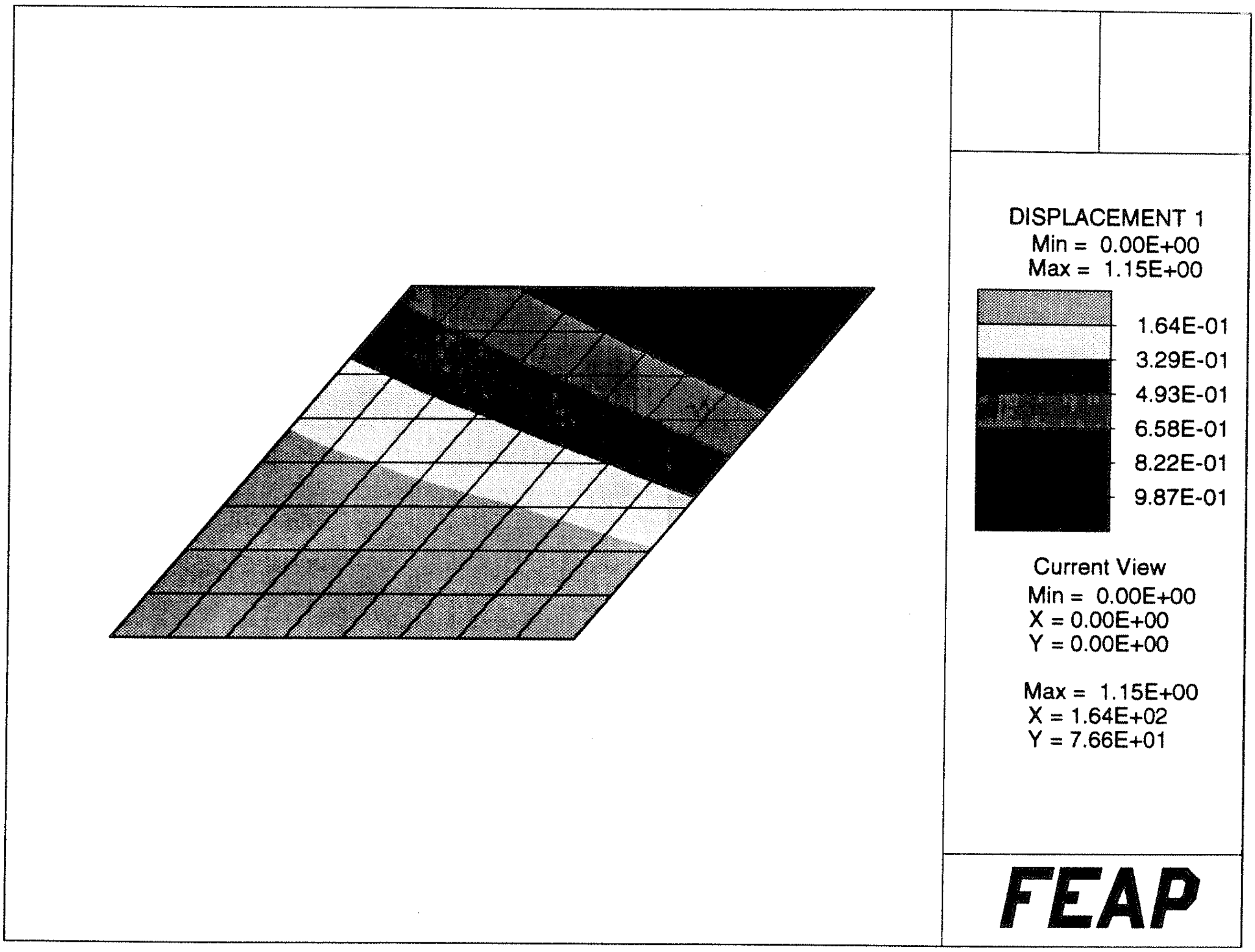

Figure 7: Typical mesh for skew cantilever plate (8×8 elements). The contour of the vertical displacement (Q4L1) is also reported.

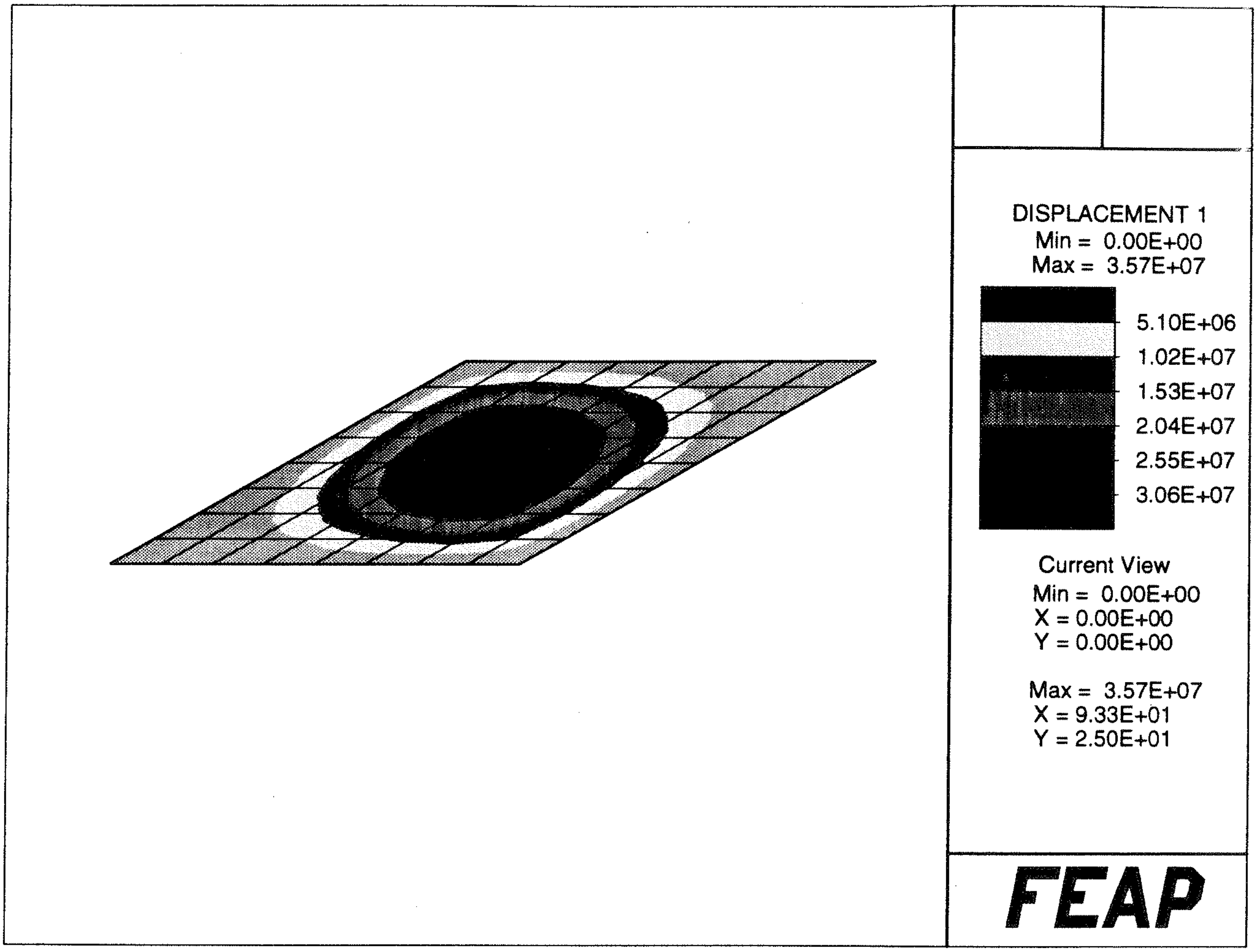

Figure 8: Typical mesh for skew simply supported plate (8×8 elements). The contour of the vertical displacement (Q4L1) is also reported.

List of Figures